

Magneto hydrodynamics of immiscible Newtonian fluids in porous regions of different variable permeability functions

Pramod Kumar Yadav^{a,*}, Sneha Jaiswal^a, Amit Kumar Verma^a, Ali J. Chamkha^b

^a Department of Mathematics, Motilal Nehru National Institute of Technology Allahabad Prayagraj, 211004, U.P, India

^b Faculty of Engineering, Kuwait College of Science and Technology, Doha District, 35004, Kuwait

ARTICLE INFO

Keywords:

Porous medium
Variable permeability
Brinkman equation
Hartmann number
Airy's function
Nield and kuznetsov function

ABSTRACT

This work is an analysis of the flow model often occurs in crude oil extraction, blood flow in the arteries, filtration of underground different fluids flowing together. In this analysis, a model of three-layered porous horizontal channel is considered. This problem is significant because of the different permeability functions used for each porous layer of the channel and flow of different Newtonian fluids takes place in these porous regions. The problem is solved for the general case which can be reduced into several particular cases. The flows inside the channel and in every porous layer is governed by the Brinkman's momentum equation for the porous medium. The momentum equations in each region of the present model are the Airy's inhomogeneous differential equations respectively. An analytical closed form solution of the flow in each region have been obtained. Authors have discussed various results of velocity profile, flow rate and wall shear stresses graphically. Our results agree with the previous published results.

1. Introduction

The flow through a composite porous layered channel meant a fluid flowing through the porous layers of different porosity and permeability placed together in a channel or duct. Such type of models has significant applications in the field of agricultural engineering, petroleum engineering, biomedical sciences, chemical engineering and frequently occurs in the recovery process of oil from petroleum reservoirs where the oil passes through different layers of sand, rock, shale, limestone that are porous in nature (Nield and Adrian, 2006; Nield and Kuznetsov, 2009; Happel and Brenner, 2012; Parvazinia et al., 2006; Rudraiah and Cheremisinoff, 1986). Porous medium is composed of some void and solid spaces, and the fluid flowing through it is governed by the Darcy's and non-Darcy's law respectively (Nield and Adrian, 2006). The various applications of porous medium led many authors to work on the research problems related to the practical applications such as in membrane filtration process of aquifers, flow through swarms of particles in the industries etc. (Yadav et al., 2010, 2013, 2017; Yadav, 2013, 2018)

The study of fluid flow through the channel filled with the porous medium gaining considerable attention of various researchers and scientist because of its occurrence in the field of recovery of fresh water

from the underground, demand to reduce power consumption in the process of recovery of oil from the earth porous layer, blood flow through the porous layered artery etc. Ansari and Deo (2017) investigated an impact of magnetic field on the flow of two-immiscible Newtonian fluids in the horizontal channel filled with the porous medium. Deo et al., 2020, 2021 have analyzed the flow behavior of micropolar fluid in the porous medium under the influence of magnetic field. Vafai and Thiyagaraja (1987) analyzed the problem of fluid flow and heat transfer through three types of interfacial problems i.e. porous-porous, porous-fluid and porous-solid interface. Allan and Hamdan (2002) considered two composite porous layers. They assumed that the flow in one porous layer is governed by Forchheimer equation and in other porous region is governed by the Brinkman equation respectively. Ford and Hamdan (1998) discussed the fluid flow through two different porous layers of a horizontal channel. An importance of fluid flow through composite porous layers has been discussed by several researchers (Wiegel, 1980; Hou et al., 1989) with various considerable practical applications which led us to discuss about the flow through the composite porous layers of variable permeability.

Nield and Kuznetsov (Nield and Kuznetsov, 2009) discussed the shear flow in a channel of variable thickness filled with the porous medium of variable permeability. Numerous problems of fluid flow

* Corresponding author.

E-mail address: pramodky@mnnit.ac.in (P.K. Yadav).

through the porous layered channel are discussed in the work (Yadav et al., 2018a, 2018b; Yadav and Jaiswal, 2018; Jaiswal and Yadav, 2019), which are of practical importance. Hamdan, (2009) had given permeability function for the Brinkman's equation governing the Poiseuille flow of viscous fluids in a horizontal channel. Hamdan and Kamel (2011), discussed about the Poiseuille flow of a fluid through a channel filled with a porous medium of variable permeability. Hill and Straughan (2008) investigated the stability of Poiseuille flow of a Newtonian fluid flowing over and through a Brinkman porous transition layer which overlies the Darcy's porous layer. Zaytoon et al. (2016a) modeled flow in the Darcy's porous layer of variable permeability. Zaytoon et al., 2016b, 2016c considered the fluid flow through a Brinkman transition porous layer of variable permeability which is sandwiched between Brinkman porous layers of constant permeability. They have evaluated velocity of fluid passing through the porous medium of variable permeability which is expressed in terms of the Nield-Kuznetsov function. Zaytoon et al. (2016d) solved the problem of flow through composite porous layers in which middle Brinkman porous layer of variable permeability is bounded by the Darcy's porous layer of constant permeability. In this work, they obtained the solution of the problem in terms of Airy's functions and the Nield-Kuznetsov function. Zaytoon et al. (2018) discussed the flow of a Newtonian fluid through a Brinkman transition layer of variable permeability which is bounded by Brinkman layer of constant permeability and clear fluid region.

Ram and Mishra (Gulab and Mishra, 1977) solved the unsteady flow of an incompressible fluid through a channel filled with porous medium under the impact of transverse magnetic field. Srivastava and Deo (2013) presented a work of fully developed flow of an incompressible and electrically conducting fluid in a channel filled with a porous medium of variable permeability under the impact of transverse applied uniform magnetic field. They have obtained a numerical solution of the problem using Galerkin's method.

In present work, authors have reviewed all the previously published model on the fluid flow through the composite porous layered channel. We found that the magnetohydrodynamics of immiscible Newtonian fluids passing through three porous layers of the channel, each porous region is of different variable permeability function, has not been discussed yet. In this paper, we have presented a model for magnetohydrodynamics fluid flow through composite porous layered channel and obtained an analytical solution of the problem in terms of an Airy's function and Nield-Kuznetsov function.

2. Description of the model and statement of the problem formulation

A model for the present problem is represented by Fig. 1. Here, a horizontal channel is formed by two parallel solid plates which are taken along X-axis. The lower plate is on the X-axis i.e. at $y^* = 0$ and upper plate is maintained at $y^* = H$, i.e. the width of horizontal channel is considered as H .

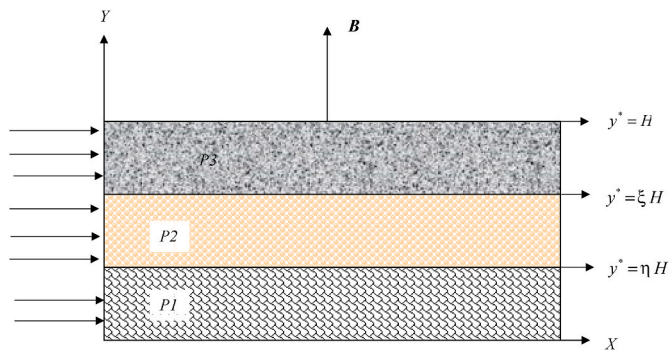


Fig. 1. Horizontal channel with composite porous layers of different widths.

To avoid confusion to the readers, let us define the three regions of channel as $P1$, $P2$ and $P3$ respectively. These regions are filled with the porous medium of different permeability and the permeability is function of y^* . It is assumed that the permeability of the porous layers varies linearly across the channel and continuous at the interfaces. There are several such literatures (Nield and Kuznetsov, 2009; Hamdan and Kamel, 2011; Zaytoon et al., 2016a, 2016b, 2016c, 2016d, 2018) that considered the linear variation of the permeability function across the channel and is known as permeability stratification. The permeability function in the porous channel varying across the channel helps to study the flow through an artificial porous media, including the design of artificial bone structures and an analysis on deformable media (such as compressed consolidated media) (Hamdan and Kamel, 2011). The permeability function chosen for the current work is given in Table 1. It is to be noted that η and ξ are any real values which help us to vary the widths of porous regions.

From the description given above, it can be observed that $K_1^*(\eta H) = K_2^*(\eta H)$ and $K_2^*(\xi H) = K_3^*(\xi H)$. Once the model has a set up as described above, an incompressible, steady and laminar flow of immiscible Newtonian fluids (F_i 's) with different viscosities (μ_i^* 's) and different electrical conductivities (σ_i^* 's) are allowed to flow along the X-axis through each porous regions separately of the channel. The subscript ' $i = 1, 2, 3$ ' is used to denote the fluids flow in the porous regions $P1$, $P2$ and $P3$ respectively. The flow inside the channel takes place due to the constant pressure gradient which is same for each porous region of the horizontal channel. An external magnetic field of uniform strength $|\mathbf{B}| = B_0$ is applied in transverse direction to the flow of fluid i.e. in vertical direction (as shown in Fig. 1).

In this section, authors have discussed about the governing equations of the flow of immiscible Newtonian fluids (F_i 's) through each porous region and their solution. Let $u_i^*(y^*)$'s be the velocity component of the corresponding F_i 's along the direction of the flow i.e. along X-axis. An induced external magnetic force due to transversally applied magnetic field with negligible induced electric current is given by $-\sigma_i^* B_0^2 u_i^*$ (Gulab and Mishra, 1977). The negative sign in the induced magnetic force represents the direction of magnetic Lorentz force which is opposite to the direction of the flow. A momentum equation along the direction of the flow of the fluid (F_i 's) in each region of the channel is expressed by Brinkman equation with an external magnetic force. So, the Brinkman equation for the flow in porous regions is given as (Zaytoon et al., 2016d):

$$\mu_{i\text{ eff}}^* \frac{d^2 u_i^*}{d y^{*2}} - \frac{\mu_i}{K_i(y^*)} u_i^* - \sigma_i^* B_0^2 u_i^* = \frac{d p^*}{d x^*} \quad (1)$$

Here $\mu_{i\text{ eff}}^*$ denotes the effective viscosities of F_i 's in their respective flow porous region and $\frac{d p^*}{d x^*}$ is pressure gradient which is taken same for each region. With the substitution of the values of $i = 1, 2 \& 3$ in Eq. (1), we get momentum equation of the fluids flowing in the regions $P1$, $P2$ & $P3$ respectively.

3. Methodology

Under this section, a methodology to obtain solution of the present problem is explained.

Following are the steps followed to achieve analytical solution of the

Table-1
Description of the porous regions of the horizontal channel presented in Fig. 1.

Porous region	Range	Width	Permeability function
$P1 (F_1, \mu_1^*, \sigma_1^*)$	$0 < y^* < \eta H$	ηH	$K_1^*(y^*) = \frac{a K_0 (\eta - \xi) H}{(y^* - \xi H)}$
$P2 (F_2, \mu_2^*, \sigma_2^*)$	$\eta H < y^* < \xi H$	$(\xi - \eta) H$	$K_2^*(y^*) = \frac{a b K_0 (\eta - \xi) H}{(b - a)y^* + (a\eta - b\xi)H}$
$P3 (F_3, \mu_3^*, \sigma_3^*)$	$\xi H < y^* < H$	$(1 - \xi) H$	$K_3^*(y^*) = \frac{b K_0 (\xi - \eta) H}{(y^* - \eta H)}$

problem:

- i. Non-dimensional forms of the governing equations.
- ii. Reducing governing equations of each porous region into standard form of differential equation.
- iii. Description on solution of standard form of differential equation.
- iv. General solution of governing equations in each porous region using previous point.
- v. Introducing mathematically and physically consistent boundary conditions.
- vi. Evaluation of arbitrary constants involved in the solution and obtaining closed form solution.

3.1. Non-dimensional governing equations of each porous region

To simplify the governing equations or to obtain dimension free solution, the following dimensionless variables are introduced:

$$y = \frac{y^*}{H} x = \frac{x^*}{H}, u_i = \frac{u_i^*}{U}, p = \frac{p^*}{\mu_i^* U/H}. \tag{2}$$

Using Eq. (2) for the variables in Table 1, we will get the description of permeability function for each porous region P1, P2 & P3 in non-dimensional form. Also, the use of non-dimensional variable defined in Eq. (2) reduces the fluid flow governing Eq. (1) in non-dimensional form for each porous region P1, P2 & P3, which is given below:

$$M_{i\text{ eff}} \frac{d^2 u_i}{d y^2} - \frac{1}{K_i(y)} u_i - Ha_i^2 u_i = \frac{1}{\alpha_i} \frac{d p}{d x}; \quad i = 1, 2, 3. \tag{3}$$

The subscript $i = 1, 2, 3$ denotes the porous region P1, P2 & P3 respectively.

Here, $M_{i\text{ eff}} = \frac{\mu_i\text{ eff}}{\mu_i}$ is an effective viscosity ratio; $K_i(y) = \frac{A}{A_i y + B_i}$ is non-dimensional permeability function where A, A_i^* and B_i^* are defined as follows:

$$A = abDa(\eta - \xi), A_i^* = \begin{cases} b, i = 1 \\ (b - a), i = 2 \text{ and } B_i^* = \begin{cases} -b\xi, i = 1 \\ a\eta - b\xi, i = 2; \\ -a\eta, i = 3 \end{cases} \\ a, i = 3 \end{cases}$$

$Da = \frac{K_0}{\mu^2}$ is known as Darcy number; $Ha_i = Ha \sqrt{\frac{\gamma_i}{\alpha_i}}$ with $Ha = B_0 H \sqrt{\frac{\sigma_1}{\mu_1}}$ is Hartmann number; $\alpha_i = \frac{\mu_i^*}{\mu_1}$ is viscosity ratio; $\gamma_i = \frac{\sigma_i}{\sigma_1}$ is an electrical conductivity ratio.

3.2. Reduction of governing equations into standard form of differential equation

In this section, authors have reduced the governing Eq. (3) for the flow of fluid in each porous region into the possible standard forms of a differential equation by using suitable transformation of variables.

Region-P1 ($0 < y < \eta$): To reduce Eq. (3) in standard form, when the fluid flow through the porous region-P1, we have used the transformation $Y_1 = \lambda_1 [(y - \xi) + a Da (\eta - \xi) Ha^2]$, where $\lambda_1 = \frac{1}{[M_{1\text{ eff}} a Da (\eta - \xi)]^{1/3}}$. Under an aforementioned transformation, the governing equation (3) for the flow of fluid through region-P1 will become as:

$$\frac{d^2 U_1}{d Y_1^2} - Y_1 U_1 = \frac{P}{\lambda_1^2 M_{1\text{ eff}}}. \tag{4}$$

Region-P2 ($\eta < y < \xi$): For the flow of fluid through the porous region P2, the transformation $Y_2 = \lambda_2 [(b - a)y + (a\eta - b\xi) + ab Da (\eta - \xi) Ha^2]$, where $\lambda_2 = \frac{1}{[M_{2\text{ eff}} a b Da (\eta - \xi)(a - b)^2]^{1/3}}$ is used to transform Eq. (3) in to standard form. In this case, the governing equation (3) will become as:

$$\frac{d^2 U_2}{d Y_2^2} - Y_2 U_2 = \frac{P}{\lambda_2^2 (b - a)^2 \alpha_1 M_{2\text{ eff}}}. \tag{5}$$

Region-P3 ($\xi < y < 1$): The governing Eq. (3) for the flow of fluid through region-P3 under the transformation $Y_3 = \lambda_3 [(y - \eta) - b Da (\xi - \eta) Ha^2]$, $\lambda_3 = \frac{1}{[M_{3\text{ eff}} b Da (\xi - \eta)]^{1/3}}$ comes out as:

$$\frac{d^2 U_3}{d Y_3^2} - Y_3 U_3 = \frac{P}{\lambda_3^2 \alpha_2 M_{3\text{ eff}}}. \tag{6}$$

It is noticed that Eqs. (4)–(6) respectively, are non-homogeneous Airy’s Differential equations (Abramowitz and Stegun, 1984) with variables Y_1, Y_2 and Y_3 .

3.3. Analytical solution of the governing equations of the problem

3.3.1. Velocities

Using the solution for the non-homogeneous Airy’s differential equation given in Appendix-A, we can write the general solution for Eqs. (4)–(6). Therefore, the general solution of Eqs. (4)–(6) for the fluid flowing in their respective porous regions are as follows:

$$U_1(Y_1) = C_1 A_i(Y_1) + C_2 B_i(Y_1) - \frac{\pi P}{\lambda_1^2 M_{1\text{ eff}}} N_i(Y_1), \tag{7}$$

$$U_2(Y_2) = C_3 A_i(Y_2) + C_4 B_i(Y_2) - \frac{\pi P}{\lambda_2^2 (b - a)^2 \alpha_1 M_{2\text{ eff}}} N_i(Y_2), \tag{8}$$

$$U_3(Y_3) = C_5 A_i(Y_3) + C_6 B_i(Y_3) - \frac{\pi P}{\lambda_3^2 \alpha_2 M_{3\text{ eff}}} N_i(Y_3). \tag{9}$$

Here, C_1, C_2, C_3, C_4, C_5 & C_6 are the arbitrary constants which are to be evaluated using mathematically and physically consistent boundary conditions. On substituting the values of $Y_1, Y_2, Y_3, \lambda_1, \lambda_2$ and λ_3 in above equations, we get the general solution of the governing equations (4)–(6) which are given below:

$$u_1(y) = C_1 A_i(\lambda_1 y + \varphi_1) + C_2 B_i(\lambda_1 y + \varphi_1) - \frac{\pi P}{\lambda_1^2 M_{1\text{ eff}}} N_i(\lambda_1 y + \varphi_1), (0 < y < \eta), \tag{10}$$

$$u_2(y) = C_3 A_i(\psi_1 y + \varphi_2) + C_4 B_i(\psi_1 y + \varphi_2) - \frac{\pi P}{\psi_1^2 \alpha_1 M_{2\text{ eff}}} N_i(\psi_1 y + \varphi_2), (\eta < y < \xi), \tag{11}$$

$$u_3(y) = C_5 A_i(\lambda_3 y + \varphi_3) + C_6 B_i(\lambda_3 y + \varphi_3) - \frac{\pi P}{\lambda_3^2 \alpha_2 M_{3\text{ eff}}} N_i(\lambda_3 y + \varphi_3), (\xi < y < 1), \tag{12}$$

where $\varphi_1 = \lambda_1 (Da (\eta - \xi) a Ha^2 - \xi)$, $\varphi_2 = \lambda_2 ((a\eta - b\xi) + ab Da (\eta - \xi) Ha^2)$, $\psi_1 = \lambda_2 (b - a)$ and $\varphi_3 = \lambda_3 (Da (\xi - \eta) b Ha^2 - \eta)$.

3.3.1.1. Asymptotic expressions of Airy’s function and Nield-Kuznetsov function

It is observed in the above sections that $\varphi_1, \varphi_2, \varphi_3$ depends on the porous layer thickness and on the Darcy numbers of the respective porous layers. For the smaller values of Darcy number, the arguments of Airy’s function and Nield-Kuznetsov function becomes larger. For large arguments, the asymptotic behavior of Airy’s and Nield-Kuznetsov function are discussed in detail by Hamdan and Kamel (2011). In this work, it is required to mention the asymptotic behavior of Airy’s and Nield-Kuznetsov function so as to obtain the analytical solution for the volumetric flow rate of the immiscible Newtonian fluids flowing in the porous layered channel. The asymptotic expressions for the Airy’s function and Nield-Kuznetsov function with large argument Z are given below in Table-2.

Using the asymptotic value of Nield-Kuznetsov function from Table-2, Eqs. 10–12 can be written as:

$$u_1(y) = C_1 A_i(\lambda_1 y + \varphi_1) + \left(C_2 + \frac{\psi_2}{3} \right) B_i(\lambda_1 y + \varphi_1), (0 < y < \eta), \tag{13}$$

Table 2

Asymptotic expressions of Airy's and Neild-Kuznetsov function for large arguments.

$A_i(Z) \approx \frac{e^{-2Z^{3/2}/3}}{2\sqrt{\pi}Z^{1/4}}$	$A'_i(Z) \approx -\frac{Z^{1/4}e^{-2Z^{3/2}/3}}{2\sqrt{\pi}}$	$\int_0^Z A_i(t) dt \approx \frac{1}{3}$
$B_i(Z) \approx \frac{e^{2Z^{3/2}/3}}{\sqrt{\pi}Z^{1/4}}$	$B'_i(Z) \approx \frac{Z^{1/4}e^{2Z^{3/2}/3}}{\sqrt{\pi}}$	$\int_0^Z B_i(t) dt \approx \frac{e^{2Z^{3/2}/3}}{\sqrt{\pi}Z^{7/4}}$
$N_i(Z) \approx -\frac{B_i(Z)}{3}$	$N'_i(Z) \approx -\frac{B'_i(Z)}{3}$	$\int_0^Z N_i(t) dt \approx -\frac{1}{3}\int_0^Z B_i(t) dt$

$$u_2(y) = C_3A_i(\psi_1y + \varphi_2) + \left(C_4 + \frac{\psi_3}{3}\right)B_i(\psi_1y + \varphi_2), (\eta < y < \xi), \tag{14}$$

$$u_3(y) = C_5A_i(\lambda_3y + \varphi_3) + \left(C_6 + \frac{\psi_4}{3}\right)B_i(\lambda_3y + \varphi_3), (\xi < y < 1), \tag{15}$$

where $\varphi_1 = \lambda_1(Da(\eta - \xi)aHa^2 - \xi)$, $\varphi_2 = \lambda_2((a\eta - b\xi) + abDa(\eta - \xi)Ha_1^2)$, $\varphi_3 = \lambda_3(Da(\xi - \eta)bHa_2^2 - \eta)$, $\psi_1 = \lambda_2(b - a)$, $\psi_2 = \frac{\pi P}{\lambda_1^2 M_{1\text{eff}}}$, $\psi_3 = \frac{\pi P}{\psi_1^2 \alpha_1 M_{2\text{eff}}}$ and $\psi_4 = \frac{\pi P}{\lambda_3^2 \alpha_2 M_{3\text{eff}}}$.

3.3.2. Volumetric flow rate

The total flow rate of the fluids flowing inside the porous channel in non-dimensional form is given by

$$Q = \int_0^\eta u_1(y) dy + \int_\eta^\xi u_2(y) dy + \int_\xi^1 u_3(y) dy. \tag{16}$$

Using Eqs. 13–15 in Eq. (16) and evaluating each integral with the help of asymptotic values of Airy's and Neild-Kuznetsov function, we get an expression for the flow rate which is given below. The details evaluation process of each term of right-hand side of Eq. (16) is discussed in Appendix-B.

$$Q = \left(\frac{C_2}{\lambda_1} + \frac{\psi_2}{3\lambda_1}\right) \left(\frac{2}{e^{\frac{2}{3}(\lambda_1\eta + \varphi_1)^{3/2}}} - \frac{2}{e^{\frac{2}{3}(\varphi_1)^{3/2}}}\right) + \frac{1}{\psi_1} \left(C_4 + \frac{\psi_3}{3}\right) \left(\frac{2}{e^{\frac{2}{3}(\psi_1\xi + \varphi_2)^{3/2}}} - \frac{2}{e^{\frac{2}{3}(\psi_1\eta + \varphi_2)^{3/2}}}\right) + \frac{1}{\lambda_3} \left(C_6 + \frac{\psi_4}{3}\right) \left(\frac{2}{e^{\frac{2}{3}(\lambda_3 + \varphi_3)^{3/2}}} - \frac{2}{e^{\frac{2}{3}(\lambda_3\xi + \varphi_3)^{3/2}}}\right). \tag{17}$$

3.3.3. Shearing stresses

The dimensionless shear stress of fluid F_1 flowing in a porous region $P1$ is given by

$$(\tau_{xy})_{P1} = \frac{d u_1}{d y}. \tag{18}$$

Using Eq. (13) in Eq. (18), we get shear stress of fluid flowing in the region $P1$ as

$$(\tau_{xy})_{P1} = \lambda_1 C_1 A'_i(\lambda_1 y + \varphi_1) + \lambda_1 C_2 B'_i(\lambda_1 y + \varphi_1) - \frac{\pi P}{\lambda_1 M_{1\text{eff}}} N'_i(\lambda_1 y + \varphi_1), (0 < y < \eta), \tag{19}$$

where prime (') over the Airy functions denotes the derivatives of respective functions.

The dimensionless shear stress of fluid F_2 flowing in a porous region $P2$ is given by

$$(\tau_{xy})_{P2} = \alpha_1 \frac{d u_2}{d y}. \tag{20}$$

Using Eq. (14) in Eq. (20), we get shear stress of fluid flowing in the region $P2$ as

$$(\tau_{xy})_{P2} = \alpha_1 \left(\psi_1 C_3 A'_i(\psi_1 y + \varphi_2) + \psi_1 C_4 B'_i(\psi_1 y + \varphi_2) - \frac{\pi P}{\psi_1 \alpha_1 M_{2\text{eff}}} N'_i(\psi_1 y + \varphi_2) \right), (\eta < y < \xi). \tag{21}$$

The dimensionless shear stress of fluid F_3 flowing in a porous region $P3$ is given by

$$(\tau_{xy})_{P3} = \alpha_2 \frac{d u_3}{d y}. \tag{22}$$

Using Eq. (15) in Eq. (22), we get shear stress of fluid flowing in the region $P3$ as

$$(\tau_{xy})_{P3} = \alpha_2 \left(\lambda_3 C_5 A'_i(\lambda_3 y + \varphi_3) + \lambda_3 C_6 B'_i(\lambda_3 y + \varphi_3) - \frac{\pi P}{\lambda_3 \alpha_2 M_{3\text{eff}}} N'_i(\lambda_3 y + \varphi_3) \right), (\xi < y < 1). \tag{23}$$

3.4. Boundary conditions

The general solution of the present problem given by Eqs. 10–12 involves six arbitrary constants which can be determined with the help of mathematically consistent and physically realistic boundary conditions. These boundary conditions in their non-dimensional form (Zaytoon et al., 2016b) are given below:

- i. No-slip condition: This condition represents the zero velocity of fluid at solid surface. For the present problem there are two solid parallel plates placed at $y = 0$ and $y = 1$, therefore the fluid flowing in the porous region $P1$ and $P3$ will have a zero velocity at the position of solid plates i.e.

$$u_1(0) = 0, \tag{24}$$

$$u_3(1) = 0. \tag{25}$$

- ii. Continuity condition: This condition is used for the continuity of fluid property at the interfaces. According to this condition, the fluid velocity and the tangential stress of two fluids respectively becomes equal to each other at their common interfaces. For the present problem, the interfaces occur at $y = \eta$ and $y = \xi$. Thus, we have

$$u_1(\eta) = u_2(\eta), \tag{26}$$

$$[(\tau_{xy})_{P1}]_{y=\eta} = [(\tau_{xy})_{P2}]_{y=\eta}, \tag{27}$$

$$u_2(\xi) = u_3(\xi), \tag{28}$$

$$[(\tau_{xy})_{P2}]_{y=\xi} = [(\tau_{xy})_{P3}]_{y=\xi} \tag{29}$$

Using Eqs. 10–12 in Eqs. 24–29, we get the values of arbitrary constants. The procedure of determining the values of arbitrary constants is presented in Appendix-B. These values are so large to present in the manuscript.

4. Results and discussion

The analysis of immiscible fluid flow through the channel of varying width is attracting the number of researchers due to its existence in various oil transportation process. In this work, we analyzed the flow behavior of immiscible Newtonian fluids which passes through the porous layered channel of varying width. Porous regions are defined by variable permeability function and flow takes place in presence of magnetic field. To avoid ambiguity in the observations of the result section of the present model, we have divided our discussion into the following parts:

- Velocity profile of immiscible Newtonian fluids at different Darcy numbers and comparison with the miscible fluids of same viscosities.
- Velocity profile of immiscible Newtonian fluids with Hartmann number and comparison with the miscible fluids of same viscosities.
- Velocity profile of immiscible Newtonian fluids at different widths of the horizontal channel and comparison with the miscible fluids of same viscosities.
- Velocity profile of immiscible Newtonian fluids with viscosity and electric conductivity ratio.
- Flow rate of the immiscible Newtonian fluids through the porous horizontal channel at very small Darcy numbers.
- Variation in wall shear stresses of immiscible Newtonian fluids at different widths, different Hartmann number and different Darcy number.

Before discussing aforementioned points, the values of several parameters involved in this work which will be helpful for the readers to understand the consistency of the problem, is presented below.

Viscosity ratios i.e. α_1 and α_2 for two different immiscible fluids can range to any real numbers except unity because at unity the condition of immiscibility of two fluids will fail. For fluid to be immiscible, their viscosity ratio should be different such as viscosity of vegetable oils and water, kerosene and water etc. Considering this fact, we have taken $\alpha_1 = 0.5$ and $\alpha_2 = 0.25$ for the immiscible fluid and $\alpha_1 = 1$ and $\alpha_2 = 1$ for miscible fluids throughout the analysis of the result.

Effective viscosity ratios i.e. $M_{1\text{eff}}$, $M_{2\text{eff}}$ and $M_{3\text{eff}}$ for fluids through the porous region will depends on the porous nature of the medium. The viscosity and effective viscosity of the fluid can be equal to each other or can less or greater than the latter.

Electrical conductivity ratios i.e. γ_1 and γ_2 are the two electrical conductivity ratios considered in the present work. When a fluid flows in the presence of magnetic field then an electric current gets induced and hence electric current flows in the fluid. Electrical conductivity of a fluid is a physical property which defines an easiness to the flow of electric currents in the fluid. The range of values for electrical conductivity ratio of the fluids can be any real numbers.

4.1. Velocity profile of immiscible Newtonian fluids at different Darcy numbers and hartmann number and comparison with the miscible fluids of same viscosities

The comparative study of non-miscible and miscible Newtonian fluid velocity in a porous layered horizontal channel at different values of Darcy number is presented in Fig. 2 (a).

From this figure, it is concluded that the continuous growth in Darcy number enhances the flow velocity of both non-miscible and miscible

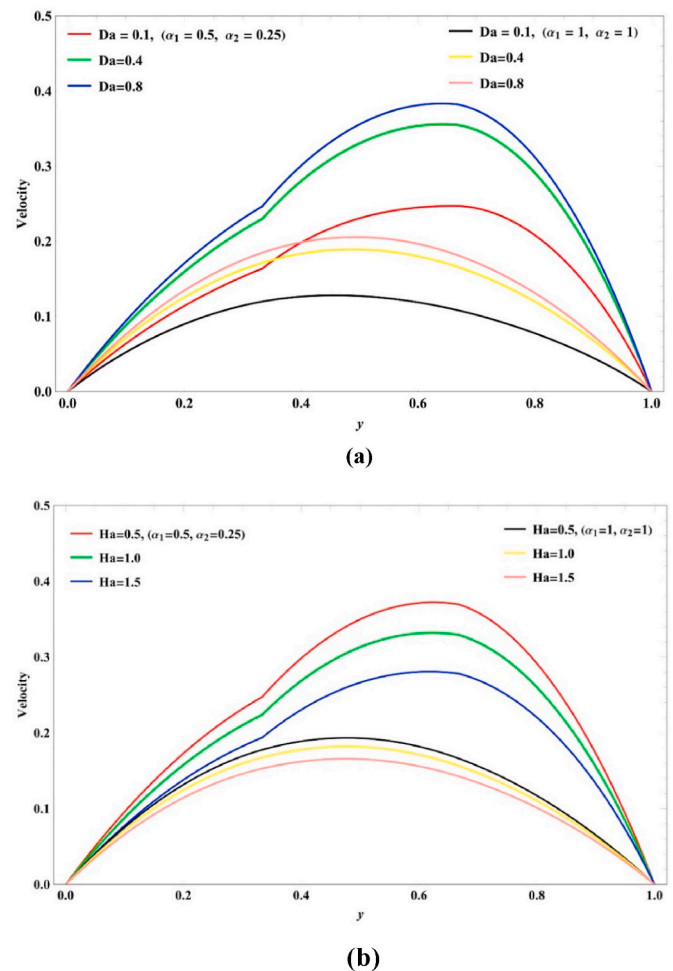


Fig. 2. (a). Variation of fluid velocity at different values of Darcy number Da when other parameters are as: $P = -2, a = 2, b = 1, M_{1\text{eff}} = 1, M_{2\text{eff}} = 1, M_{3\text{eff}} = 1, \gamma_1 = 1, \gamma_2 = 1.2, \eta = 1/3, \xi = 2/3, Ha = 1$ Fig. 2 (b). Variation of fluid velocity at different values of Hartmann number Ha when other parameters are as: $P = -2, a = 2, b = 1, M_{1\text{eff}} = 1, M_{2\text{eff}} = 1.2, M_{3\text{eff}} = 1.4, \gamma_1 = 1, \gamma_2 = 1.2, \eta = 1/3, \xi = 2/3, Da = 1$

Newtonian fluids in porous layered channel. Fig. 2 (a) demonstrates that the Darcy number shows much impact on the velocity of non-miscible Newtonian fluid flow in upper porous layered of the channel as comparison to the bottom porous layer, however, the velocity of miscible Newtonian fluid in all the porous layered of the channel is uniformly impacted by Darcy number. During analysis of the result, a remarkable conclusion is made which is non-miscible Newtonian fluid velocity always received higher values in all the porous layered horizontal channel as compared to the velocity of miscible Newtonian fluid. The similar kind of variation was observed in the previous work of Zaytoon et al., 2016b, 2016c, 2016d, 2018. Fig. 2 (b) is prepared to visualize the impact of Hartmann number on the flow velocity of immiscible and miscible Newtonian fluids in a porous layered channel. From this figure, it is concluded that the flow velocity of immiscible and miscible both Newtonian fluids in a porous layered channel decreases on increasing the Hartmann number i.e. on increasing the strength of applied uniform magnetic field. It is also noticed from this figure that the applied uniform magnetic field shows much impact on the flow velocity of immiscible Newtonian fluids as compared to miscible Newtonian fluids.

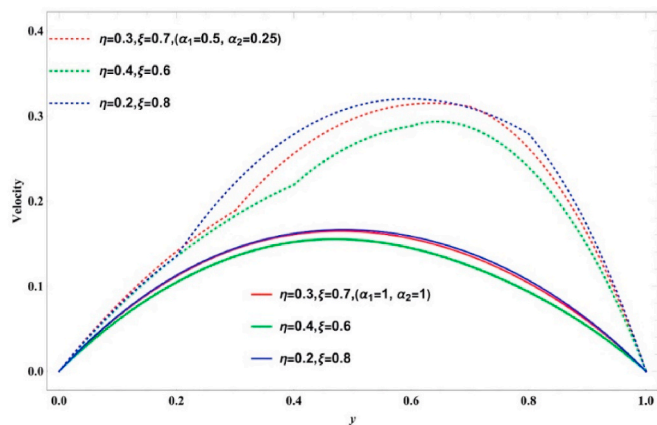


Fig. 3. Variation of fluid velocity with widths of the horizontal channel when other parameters are as: $P = -2, a = 2, b = 1, M_{1\text{eff}} = 1, M_{2\text{eff}} = 1, M_{3\text{eff}} = 1, \gamma_1 = 1, \gamma_2 = 1.2, Da = 0.2, Ha = 1$

4.2. Velocity profile of immiscible Newtonian fluids at different widths of the horizontal channel and comparison with the miscible fluids of same viscosities

This subsection displays the impact of porous layered widths of horizontal channel on the velocity profile of non-miscible Newtonian fluids passing through channel and its comparison with the miscible Newtonian fluids velocity in channel having same viscosities as of non-miscible Newtonian fluids. Fig. 3 depicts that the width of porous layer can be used to manage the velocity of miscible and non-miscible Newtonian fluids in a porous channel. From this figure, it is concluded that the miscible and non-miscible Newtonian fluids velocity in each porous region of the horizontal channel get reduced on decreasing the width of middle porous layer (Fig. 3).

4.3. Velocity profile of immiscible Newtonian fluids with viscosity and electric conductivity ratio

This subsection aims to explore the influence of viscosity, effective viscosity and electric conductivity ratio parameter on the velocity profile of immiscible Newtonian fluids which takes place through a horizontal porous channel. The graphical representation of velocity profile with viscosity ratios parameter α_1 and α_2 is shown in supplementary material (Figs. S1 and S2 respectively). From the graphs, authors concluded that the velocity of immiscible Newtonian fluids decreases on

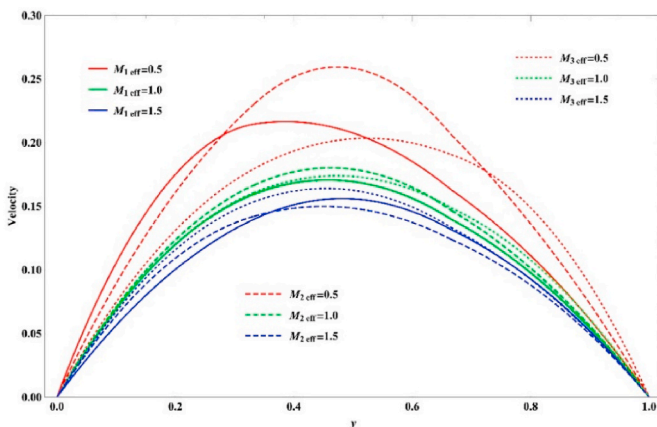


Fig. 4. Variation of fluid velocity with effective viscosity ratios $M_{1\text{eff}}, M_{2\text{eff}}$ and $M_{3\text{eff}}$ when other parameters are as: $P = -2, a = 2, b = 1, \alpha_1 = 1, \alpha_2 = 1.2, \gamma_1 = 1, \gamma_2 = 1.2, \eta = 1/3, \xi = 2/3, Da = 1, Ha = 1$

increasing the viscosity ratio parameter α_2 throughout the horizontal porous channel and this effect is maximum near the middle of the channel, however, the viscosity ratio parameter α_1 shows the effect on velocity only near the middle of the channel. During the analysis of the results, it is also noticed that the velocity profile of immiscible Newtonian fluids get reduced on enhancing the electric conductivity ratio γ_1 (Fig. S3), but electric conductivity ratio γ_2 does not shows much effect on the non-miscible Newtonian fluid velocity in the channel.

The changes in flow velocity of non-miscible fluid inside a porous channel with respect to effective viscosity ratio $M_{1\text{eff}}, M_{2\text{eff}}$ and $M_{3\text{eff}}$ is illustrated in Fig. 4. In Fig. 4, solid lines show the effect of effective viscosity ratio $M_{1\text{eff}}$ when $M_{2\text{eff}} = 1.2$ and $M_{3\text{eff}} = 1.4$; dashed lines show the effect of effective viscosity ratio $M_{2\text{eff}}$ when $M_{1\text{eff}} = 1$ and $M_{3\text{eff}} = 1.4$; and dotted lines show the effect of effective viscosity ratio $M_{3\text{eff}}$ when $M_{1\text{eff}} = 1$ and $M_{2\text{eff}} = 1.2$. This figure clearly indicates that the flow velocity of non-miscible fluid gets reduced on enhancing the effective viscosity ratios. From this figure, it is also concluded that small values of effective viscosity ratio $M_{2\text{eff}}$ shows much effect on flow velocity of non-miscible fluid in all the porous region of the channel as compared to other effective viscosity ratios $M_{1\text{eff}}$ and $M_{3\text{eff}}$.

4.4. Flow rate of the immiscible Newtonian fluids through the porous horizontal channel at various emerging fluid parameters

This subsection represents the influence of various existing non-dimensional fluid parameters on the flow rate of non-miscible Newtonian fluid in a horizontal porous channel. The flow rate of non-miscible Newtonian fluid for various numerical values of small Darcy numbers is illustrated in Fig. 5. From this figure, it is observed that the flow rate of non-miscible fluid in porous channel get enhanced on increasing the Darcy numbers. From Fig. 5, we also concluded that the very small values of Darcy numbers show negligible impact on the flow rate of immiscible fluids, however, the small values of viscosity ratio α_1 show much impact on it.

Fig. 6 depicts the variation of flow rate with viscosity ratio α_2 at different values of the Hartman number (Ha). From this figure, it is noticed that the flow rate of non-miscible Newtonian fluid in porous channel get enhanced on decreasing the Hartmann number (Ha). It is important to mention that the small values of Hartmann number show much impact on the flow rate, however, viscosity ratio α_2 show very less impact on it. The variation of the flow rate with the effective viscosity ratios ($M_{1\text{eff}}, M_{2\text{eff}}$) and electric conductive ratios (γ_1, γ_2) are presented in Figs. 7 and 8 respectively. From these figures, it is noticed that the flow rate increases on increasing the effective viscosity ratios $M_{1\text{eff}}$ and

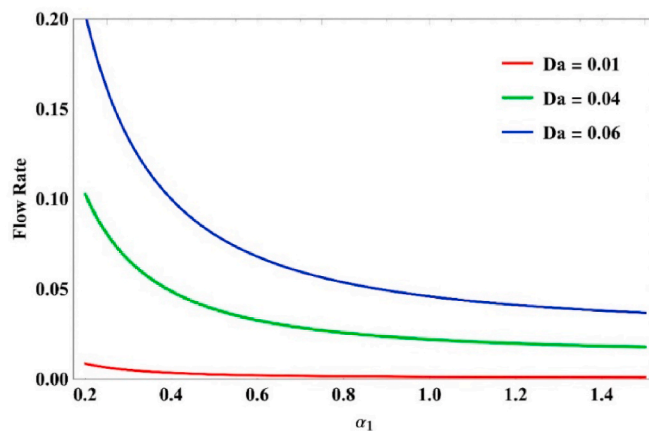


Fig. 5. Variation of flow rate with viscosity ratio α_1 at different values of the Darcy number (Da) when other parameters are as: $P = -2, a = 2, b = 1, M_{1\text{eff}} = 0.4, M_{2\text{eff}} = 0.6, M_{3\text{eff}} = 1, \alpha_2 = 0.25, \gamma_1 = 0.8, \gamma_2 = 1, \eta = 1/3, \xi = 2/3, Ha = 0.2$.

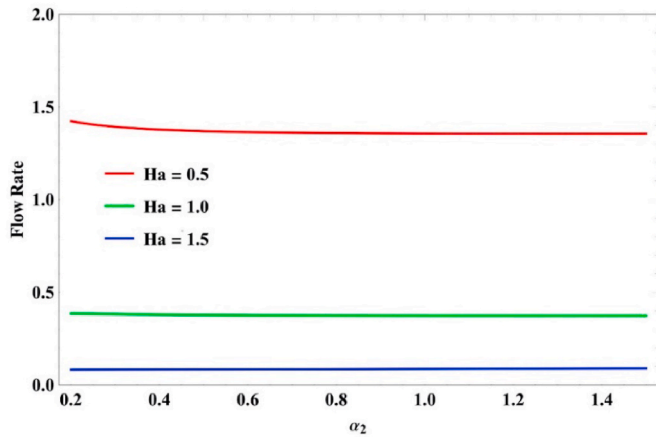


Fig. 6. Variation of flow rate with viscosity ratio α_2 at different values of the Hartmann number (Ha) when other parameters are as: $P = -2, a = 2, b = 1, M_{1\text{eff}} = 0.4, M_{2\text{eff}} = 0.6, M_{3\text{eff}} = 1, \alpha_1 = 0.5, \gamma_1 = 0.8, \gamma_2 = 1, \eta = 1/3, \xi = 2/3, Da = 0.5$.

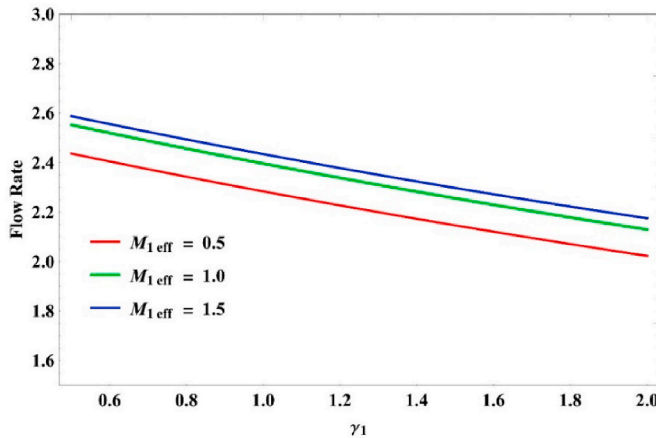


Fig. 7. Variation of flow rate with electric conductivity ratio γ_1 at different values of the effective viscosity ratio $M_{1\text{eff}}$ when other parameters are as: $P = -2, a = 2, b = 1, M_{2\text{eff}} = 0.6, M_{3\text{eff}} = 1, \alpha_1 = 0.5, \alpha_2 = 0.25, \gamma_2 = 1, \eta = 1/3, \xi = 2/3, Ha = 0.2, Da = 0.5$.

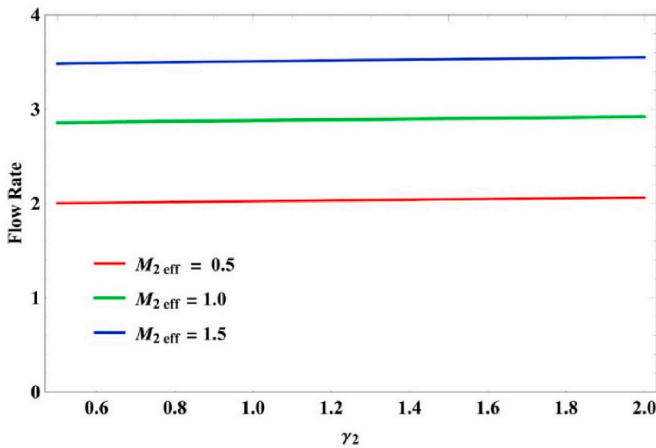


Fig. 8. Variation of flow rate with electric conductivity ratio γ_2 at different values of the effective viscosity ratio $M_{2\text{eff}}$ when other parameters are as: $P = -2, a = 2, b = 1, M_{1\text{eff}} = 0.4, M_{3\text{eff}} = 1, \alpha_1 = 0.5, \alpha_2 = 0.25, \gamma_1 = 1, \eta = 1/3, \xi = 2/3, Ha = 0.2, Da = 0.5$.

Table 3

Numerical value of wall shear stress at $y = 0$ for different widths, Hartmann and Darcy number.

		Wall shear stress $(\tau_{xy})_{p_1}$ at $y = 0$		
		Da = .01	Da = 0.05	Da = 0.5
$P = -2, a = 2, b = 1,$ $\gamma_1 = 1, \gamma_2 = 1.2,$ $M_{1\text{eff}} = 1, M_{2\text{eff}} = 0.6$	$\eta = 0.4, \xi = 0.6$	0.19015761	0.481473487	0.929262518
	$1.2, M_{3\text{eff}} = 1.4,$ $\alpha_1 = 0.5, \alpha_2 = 0.25, Ha = 0.2$	0.250243255	0.560019096	0.927745589
	$\eta = 0.7$	0.283204115	0.568340128	0.879138175
$P = -2, a = 2, b = 1,$ $\gamma_1 = 1, \gamma_2 = 1,$ $M_{1\text{eff}} = 1, M_{2\text{eff}} = 1.2, M_{3\text{eff}} = 1.4,$ $\alpha_1 = 0.5, \alpha_2 = 0.25, \eta = 1/3, \xi = 2/3$	$0.2, \xi = 0.8$	0.235999192	0.562458292	1.007693345
	$Ha = 0.5$	0.234487864	0.545442481	0.937552559
	$Ha = 1.0$	0.232043906	0.520202536	0.844950985
	1.5			

Table 4

Numerical value of wall shear stress at $y = 1$ for different widths, Hartmann and Darcy Number.

		Wall shear stress $(\tau_{xy})_{p_3}$ at $y = 1$		
		Da = .01	Da = 0.05	Da = 0.5
$P = -2, a = 2, b = 1,$ $\gamma_1 = 1, \gamma_2 = 1.2,$ $M_{1\text{eff}} = 1, M_{2\text{eff}} = 0.6$	$\eta = 0.4, \xi = 0.6$	0.107852272	0.242593135	0.4205327
	$1.2, M_{3\text{eff}} = 1.4,$ $\alpha_1 = 0.5, \alpha_2 = 0.25, Ha = 1$	0.13679298	0.278883806	0.446859315
	$\eta = 0.7$	0.144510216	0.290420795	0.483169261
$P = -2, a = 2, b = 1,$ $\gamma_1 = 1, \gamma_2 = 1,$ $M_{1\text{eff}} = 1, M_{2\text{eff}} = 1.2, M_{3\text{eff}} = 1.4,$ $\alpha_1 = 0.5, \alpha_2 = 0.25, \eta = 1/3, \xi = 2/3$	$0.2, \xi = 0.8$	0.131691424	0.283896305	0.480454509
	$Ha = 0.5$	0.130435847	0.273553852	0.443200712
	$Ha = 1.0$	0.128421927	0.258368481	0.394473453
	1.5			

$M_{2\text{eff}}$ both and decrease on increasing the electric conductive ratio γ_1 . The electric conductivity ratio γ_2 does not show much impact on flow rate (Fig. 8).

4.5. Variation in wall shear stresses of immiscible Newtonian fluids at different widths, different hartmann number and different Darcy number

In this subsection, authors have presented the numerical data of the wall shear stresses at the different values of the non-dimensional parameters. Table 3 and Table 4 are prepared to visualize the impact of Hartmann number, Darcy number and different widths of porous layers of the channel on the shear stresses at the lower and upper wall of the channel respectively. Tables 3 and 4 depict that the shear stresses at the lower and upper walls of the channel get enhanced on increasing the Darcy number. It is noticed from these tables that the use of high strength magnetic field diminishes the shear stresses at both walls of the channel. These tables also made an important observation that the stresses at both the wall of the channel can be reduce by decreasing the width of the middle porous layer of the channel.

Table 5 and Table 6 present the behavior of wall shear stresses at lower and upper wall of the channel respectively with various values of the electric conductivity ratios and viscosity ratios. These tables confirm

Table 5

Numerical value of wall shear stress at $y = 0$ for different values of electric conductivity and viscosity ratio.

		Wall shear stress $(\tau_{xy})_{P_1}$ at $y = 0$		
		Da = 0.01	Da = 0.05	Da = 0.1
$P = -2, a = 2,$ $b = 1, \gamma_1 = 1,$ $\gamma_2 = 1.2, \alpha_2 =$ $0.25, \xi = 2/3$ $M_1 \text{ eff} = 1,$ $M_2 \text{ eff} = 1.2, \eta =$ $1/3, M_3 \text{ eff} =$ $1.4Ha = 1$	α_1 0.5	0.234483419	0.545108965	0.701077634
	1.0	0.226470276	0.507197161	0.663705838
	1.5	0.221316048	0.476872765	0.627548434
$P = -2, a = 2,$ $b = 1, \gamma_1 = 1,$ $\gamma_2 = 1.2, \alpha_1 =$ $0.5, \xi = 2/3$ $M_1 \text{ eff} = 1,$ $M_2 \text{ eff} = 1.2, \eta =$ $1/3, M_3 \text{ eff} =$ $1.4Ha = 1$	α_2 0.5	0.234483419	0.545108965	0.701077634
	1.0	0.233910419	0.52818782	0.666785162
	1.5	0.23333674	0.511505488	0.633332977
$P = -2, a = 2,$ $b = 1, \xi = 2/3$ $\gamma_2 = 1.2, \alpha_1 =$ $0.5, \alpha_2 = 0.25,$ $M_1 \text{ eff} = 1,$ $M_2 \text{ eff} = 1.2, \eta =$ $1/3, M_3 \text{ eff} =$ $1.4Ha = 1$	γ_1 0.5	0.234677809	0.549948654	0.711583172
	1.0	0.234487864	0.545442481	0.701934295
	1.5	0.234300885	0.54113173	0.692836673
$P = -2, a = 2,$ $b = 1, \gamma_1 = 1,$ $\alpha_1 = 0.5, \alpha_2 =$ $0.25, \xi = 2/3$ $M_1 \text{ eff} = 1,$ $M_2 \text{ eff} = 1.2, \eta =$ $1/3, M_3 \text{ eff} =$ $1.4Ha = 1$	γ_2 0.5	0.234499095	0.546297495	0.704143972
	1.0	0.234487864	0.545442481	0.701934295
	1.5	0.234476802	0.544617452	0.699820485

that the shear stresses at lower and upper wall of the porous channel can be reduced on increasing the electric conductivity ratios γ_1 and γ_2 both. From these tables, it is also concluded that the increase in viscosity ratio diminishes the wall shear stress at the lower wall of the porous channel, however, viscosity ratio α_2 may use to boost up the shear stress at the upper wall of the porous channel.

5. Particular case

Let us assume that the viscosities μ_i^* and conductivities σ_i^* of the considered immiscible fluids in the present model are same and the non-dimensional form of the permeability function in three regions are defined as follows:

$$K_i(y) = \begin{cases} a, & i = 1 \\ \frac{ab(\eta - \xi)}{(b-a)y + (a\eta - b\xi)}, & i = 2 \\ b, & i = 3, \end{cases} \quad (30)$$

Therefore, the velocity of Newtonian fluid flowing through each of the porous regions $P1, P2$ and $P3$ respectively, comes out as:

$$u_1(y) = C_1 \exp\left(\sqrt{\lambda_1^2 + Ha^2}\right)y + C_2 \exp\left(-\sqrt{\lambda_1^2 + Ha^2}\right)y - \frac{P}{(\lambda_1^2 + Ha^2)M_1 \text{ eff}}, \quad (0 < y < \eta), \quad (31)$$

$$u_2(y) = C_3A_i \left(\lambda_2 [(b-a)y + (a\eta - b\xi)] + ab Da (\eta - \xi) Ha^2 \right) + C_4B_i \left(\lambda_2 [(b-a)y + (a\eta - b\xi)] + ab Da (\eta - \xi) Ha^2 \right) - \frac{\pi P}{\lambda_2^2 (b-a)^2 \alpha_1 M_2 \text{ eff}} N_i \left(\lambda_2 [(b-a)y + (a\eta - b\xi)] + ab Da (\eta - \xi) Ha^2 \right), \quad (\eta < y < \xi), \quad (32)$$

Table 6

Numerical value of wall shear stress at $y = 1$ for different values of electric conductivity and viscosity ratio.

		Wall shear stress $(\tau_{xy})_{P_3}$ at $y = 1$		
		Da = 0.01	Da = 0.05	Da = 0.1
$P = -2, a = 2, b =$ $1, \gamma_1 = 1,$ $\gamma_2 = 1.2, \alpha_2 =$ $0.25, \xi = 2/3$ $M_1 \text{ eff} = 1,$ $M_2 \text{ eff} = 1.2, \eta =$ $1/3, M_3 \text{ eff} =$ $1.4Ha = 1$	α_1 0.5	0.130128404	0.271669134	0.338808234
	1.0	0.127255729	0.249507915	0.309269728
	1.5	0.125956686	0.237901295	0.292840182
$P = -2, a = 2, b =$ $1, \gamma_1 = 1,$ $\gamma_2 = 1.2, \alpha_1 =$ $0.5, \xi = 2/3$ $M_1 \text{ eff} = 1,$ $M_2 \text{ eff} = 1.2, \eta =$ $1/3, M_3 \text{ eff} =$ $1.4Ha = 1$	α_2 0.5	0.130128404	0.271669134	0.338808234
	1.0	0.134951634	0.315588619	0.408990533
	1.5	0.139392083	0.357381501	0.475486903
$P = -2, a = 2, b =$ $1, \xi = 2/3$ $\gamma_2 = 1.2, \alpha_1 =$ $0.5, \alpha_2 = 0.25,$ $M_1 \text{ eff} = 1,$ $M_2 \text{ eff} = 1.2, \eta =$ $1/3, M_3 \text{ eff} =$ $1.4Ha = 1$	γ_1 0.5	0.130488231	0.275236	0.34558727
	1.0	0.130435847	0.273553852	0.341843008
	1.5	0.130384315	0.271946307	0.338316142
$P = -2, a = 2, b =$ $1, \gamma_1 = 1,$ $\alpha_1 = 0.5, \alpha_2 =$ $0.25, \xi = 2/3$ $M_1 \text{ eff} = 1,$ $M_2 \text{ eff} = 1.2, \eta =$ $1/3, M_3 \text{ eff} =$ $1.4Ha = 1$	γ_2 0.5	0.131213349	0.278396712	0.349690713
	1.0	0.130435847	0.273553852	0.341843008
	1.5	0.129670986	0.268896121	0.33436271

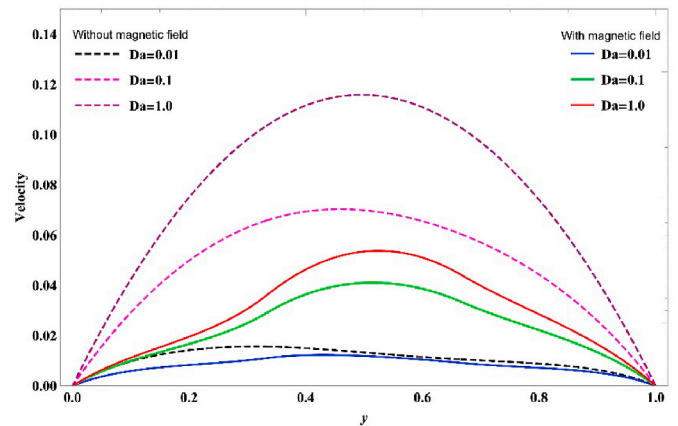


Fig. 9. Variation in Newtonian fluid velocity with different values of Darcy number Da when other parameters are as: $P = -1, a = 2, b = 1, M_1 \text{ eff} = 1, M_2 \text{ eff} = 1, M_3 \text{ eff} = 1, \gamma_1 = 0.5, \gamma_2 = 0.5, \eta = 1/3, \xi = 2/3, Ha = 8$.

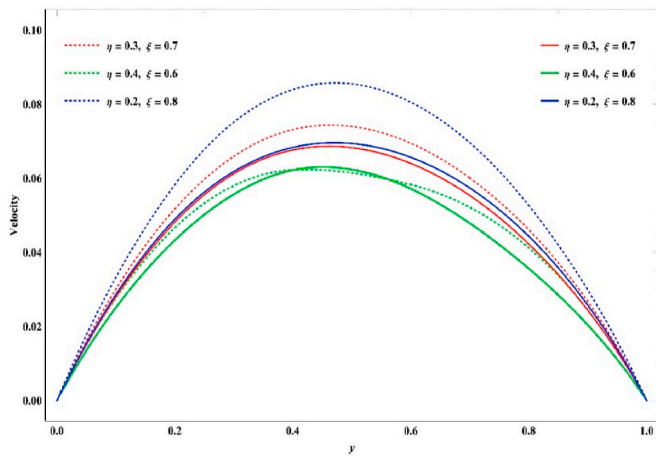


Fig. 10. Comparison of flow behavior in porous region of variable permeability with the flow in porous region of constant permeability at different widths of the porous regions of the horizontal channel when other parameters are as: $P = -1, a = 2, b = 1, M_{1\text{eff}} = 1, M_{2\text{eff}} = 1, M_{3\text{eff}} = 1, \gamma_1 = 0.5, \gamma_2 = 0.5, Da = 0.1, Ha = 0.2$.

$$u_3(y) = C_5 \exp\left(\sqrt{\lambda_3^2 + Ha^2}\right)y + C_2 \exp\left(-\sqrt{\lambda_3^2 + Ha^2}\right)y - \frac{P}{(\lambda_3^2 + Ha^2)M_{3\text{eff}}}, (\xi < y < 1). \tag{33}$$

Here, $\lambda_1^2 = \frac{1}{a Da M_{1\text{eff}}}, \lambda_2 = \frac{1}{|M_{2\text{eff}} a b Da (\eta - \xi)(a - b)^2|^{1/3}}, \lambda_3^2 = \frac{1}{b Da M_{3\text{eff}}}$ and all other parameters are same as defined in section 3.1.

At the limiting value $Ha \rightarrow 0$ i.e. in the absence of magnetic field, the velocity of Newtonian fluid in each porous regions $P1, P2$ and $P3$ respectively, will becomes as:

$$u_1(y) = C_1 \exp(\lambda_1)y + C_2 \exp(-\lambda_1)y - \frac{P}{\lambda_1^2 M_{1\text{eff}}}, (0 < y < \eta), \tag{34}$$

$$u_2(y) = C_3 A_i \left(\lambda_2 \left[(b - a)y + (a\eta - b\xi) \right] \right) + C_4 B_i \left(\lambda_2 \left[(b - a)y + (a\eta - b\xi) \right] \right) - \frac{\pi P}{\lambda_2^2 (b - a)^2 M_{2\text{eff}}} N_i \left(\lambda_2 \left[(b - a)y + (a\eta - b\xi) \right] \right), (\eta < y < \xi), \tag{35}$$

$$u_3(y) = C_5 \exp(\lambda_3)y + C_2 \exp(-\lambda_3)y - \frac{P}{\lambda_3 M_{3\text{eff}}}, (\xi < y < 1). \tag{36}$$

For the particular value of pressure gradient $P = -1$, these results agree with the work of Zaytoon et al. (2016b).

The variation in velocity profile of Newtonian fluid flowing through composite porous layered channel with different Darcy's number and width of the porous regions is presented in Figs. 9 and 10 respectively. Solid lines in Fig. 9 shows the variation in velocity profile of Newtonian fluid flowing through composite porous layered channel in presence of magnetic field. However, dashed lines show the variation in velocity profile of Newtonian fluid in absence of magnetic field which agrees with the result of Zaytoon et al. (2016b).

Fig. 10 depicts the comparison in flow velocity of Newtonian fluids in the porous regions of the variable permeability (present work) with the flow velocity of Newtonian fluids in the porous regions of the constant permeability (Zaytoon et al. (2016b)). The dotted lines in Fig. 10 represent the flow velocity in porous region of constant permeability while the solid lines represent the flow velocity in porous region of variable permeability at different widths. From this figure, it is observed that velocity of the fluids flowing through the porous region of variable

permeability have lower values as compared with the velocity of the fluids in the porous region of constant permeability. Hence, it is concluded that an effect of considering porous medium of variable permeability is significant.

6. Conclusion

This work has explained the flow behavior, flow rate and shear stresses at the walls of the channel when the three non-miscible Newtonian fluids taking place in a three-layered porous horizontal channel under the presence of uniform magnetic field. Each porous layer of the channel having different permeability functions. Such problem of three different variable permeability functions with three immiscible Newtonian fluid flow in the presence of magnetic field has not been discussed yet. The results obtained for the considered problem can be used in the filtration process of different underground fluid, extraction of crude oil, etc. In this work, the effects of various existing non-dimensional parameters on the fluid velocity, flow rate and wall shear stresses are investigated and presented in graphical and tabular form. The present study is very helpful for those engineers, scientists, and industrial community who are working on the non-miscible fluid. The points concluded from the present analysis are as follows:

- Darcy number (Da) raised the velocity, flow rate as well as shear stresses at the wall when the three non-miscible Newtonian fluids passing through different porous layered horizontal channel.
- Immiscible nature of Newtonian fluids achieved higher values of velocity in all the variable permeability porous layered horizontal channel as comparison to the miscible nature of Newtonian fluids.
- Width of middle porous layer of the horizontal channel can be used to control the velocity and shear stresses acting at the wall of the channel because of the non-miscible nature of Newtonian fluids flow.
- Use of the uniform magnetic field in the considered problem reduces the velocity of immiscible and miscible both nature of Newtonian fluids in the porous channel.
- Electric conductivity and viscosity ratio both reduces the velocity of non-miscible Newtonian fluids in the channel. It is also concluded that these parameters can be used in controlling of shear stresses at the wall of the porous horizontal channel.
- The velocity of immiscible/miscible nature of Newtonian fluid passing through porous region with permeability of variable nature has lower values as compared to the velocity of immiscible/miscible nature of Newtonian fluid passing through porous region of constant permeability.

Credit author statement

Pramod Kumar Yadav: Supervision, Conceptualization, Methodology, Reviewing and Editing. Sneha Jaiswal: Modelling, Methodology, Writing – original draft. Amit Kumar Verma: Software, preparation of graphs and Investigation of result. Ali J. Chamkha: Conceptualization, Writing- Reviewing and Editing.

Declaration of competing interest

The authors declare that they have no known competing financial interests or personal relationships that could have appeared to influence the work reported in this paper.

Data availability

No data was used for the research described in the article.

Acknowledgement

Authors are grateful to the reviewers for their valuable suggestions

that led to much improvement in the presentation of the manuscript. The second author is thankful to Council of Scientific and Industrial Research

CSIR New Delhi, India for the financial support under the file no. 09/1032(0021)/2020-EMR-I.

Appendix A. Supplementary data

Supplementary data to this article can be found online at <https://doi.org/10.1016/j.petrol.2022.111113>.

Appendix-A

Solution of non-homogeneous Airy’s differential equation.

In this section, we have shown the general solution of the non-homogeneous Airy’s differential equation (Abramowitz and Stegun, 1984):

$$\frac{d^2w}{dz^2} - zw = Q, \tag{A.1}$$

where $w(z)$ is depending on an independent variable z and Q is any constant.

The solution of homogeneous part of Eq. (A.1) is given by two linearly independent functions $A_i(z)$ and $B_i(z)$ which are known as Airy’s functions (Abramowitz and Stegun, 1984). The particular integral of Eq. (A.1) is found using method of variation of parameters. Therefore, particular integral (P.I.) of Eq. (A.1) is given as (Nield and Kuznetsov, 2009; Hill and Straughan, 2008; Zaytoon et al., 2016c):

$$P.I. = -\pi Q N_i(z), \tag{A.2}$$

$$here N_i(z) = A_i(z) \int_0^z B_i(t) dt - B_i(z) \int_0^z A_i(t) dt, \tag{A.3}$$

and is known as Nield- Kuznetsov function which is defined in the work of Nield and Kuznetsov (2009) and extensively studied by Hamdan and Kamel (Hill and Straughan, 2008).

Therefore, the general solution of non-homogeneous Airy’s differential equation (A.1) is given as:

$$w(z) = c_1 A_i(z) + c_2 B_i(z) - \pi Q N_i(z), \tag{A.4}$$

where c_1 & c_2 are arbitrary constants.

Appendix-B

$$\int_0^\eta u_1(y) dy = \int_0^\eta \left(C_1 A_i(\lambda_1 y + \varphi_1) + \left(C_2 + \frac{\psi_2}{3} \right) B_i(\lambda_1 y + \varphi_1) \right) dy. \tag{B.1}$$

Let $t = \lambda_1 y + \varphi_1$, then $dt = \lambda_1 dy$ then Eq.(B.1) becomes

$$\int_0^\eta u_1(y) dy = \frac{1}{\lambda_1} \int_{\varphi_1}^{\lambda_1 \eta + \varphi_1} \left(C_1 A_i(t) + \left(C_2 + \frac{\psi_2}{3} \right) B_i(t) \right) dt, \tag{B.2}$$

where

$$\int_{\varphi_1}^{\lambda_1 \eta + \varphi_1} A_i(t) dt = \int_{\varphi_1}^0 A_i(t) dt + \int_0^{\lambda_1 \eta + \varphi_1} A_i(t) dt = - \int_0^{\varphi_1} A_i(t) dt + \int_0^{\lambda_1 \eta + \varphi_1} A_i(t) dt. \tag{B.3}$$

Using asymptotic value of Airy’s function from table-2 i.e. $\int_0^z A_i(t) dt \approx \frac{1}{3}$ in Eq. (B.3), we get

$$\int_{\varphi_1}^{\lambda_1 \eta + \varphi_1} A_i(t) dt = 0 \tag{B.4}$$

Similarly, we have

$$\int_{\varphi_1}^{\lambda_1 \eta + \varphi_1} B_i(t) dt = \int_{\varphi_1}^0 B_i(t) dt + \int_0^{\lambda_1 \eta + \varphi_1} B_i(t) dt = - \int_0^{\varphi_1} B_i(t) dt + \int_0^{\lambda_1 \eta + \varphi_1} B_i(t) dt. \tag{B.5}$$

Using asymptotic value of Airy’s function from table-2 i.e. $\int_0^z B_i(t) dt \approx \frac{e^{2Z^{3/2}/3}}{\sqrt{\pi Z^{7/4}}}$ in Eq. (B.5), we get

$$\int_{\varphi_1}^{\lambda_1 \eta + \varphi_1} B_i(t) dt = \frac{e^{\frac{2}{3}(\lambda_1 \eta + \varphi_1)^{3/2}}}{\sqrt{\pi}(\lambda_1 \eta + \varphi_1)^{7/4}} - \frac{e^{\frac{2}{3}(\varphi_1)^{3/2}}}{\sqrt{\pi}(\varphi_1)^{7/4}}. \tag{B.6}$$

Using Eqs. (B.4) and (B.6) in Eq. (B.2), we get

$$\int_0^\eta u_1(y) dy = \left(\frac{C_2}{\lambda_1} + \frac{\Psi_2}{3\lambda_1} \right) \left(\frac{e^{\frac{2}{3}(\lambda_1 \eta + \varphi_1)^{3/2}}}{\sqrt{\pi}(\lambda_1 \eta + \varphi_1)^{7/4}} - \frac{e^{\frac{2}{3}(\varphi_1)^{3/2}}}{\sqrt{\pi}(\varphi_1)^{7/4}} \right). \tag{B.7}$$

Now, $\int_\eta^\xi u_2(y) dy$ can be written as follows:

$$\int_\eta^\xi u_2(y) dy = \int_0^\xi u_2(y) dy - \int_0^\eta u_2(y) dy. \tag{B.8}$$

From Eq. (14) we have

$$\int_\eta^\xi u_2(y) dy = \int_0^\xi \left(C_3 A_i(\psi_1 y + \varphi_2) + \left(C_4 + \frac{\Psi_3}{3} \right) B_i(\psi_1 y + \varphi_2) \right) dy - \int_0^\eta \left(C_3 A_i(\psi_1 y + \varphi_2) + \left(C_4 + \frac{\Psi_3}{3} \right) B_i(\psi_1 y + \varphi_2) \right) dy. \tag{B.9}$$

Solving RHS of Eq. (B.9) by considering $t = \psi_1 y + \varphi_2$, we have

$$\int_\eta^\xi u_2(y) dy = \frac{1}{\psi_1} \left(\int_{\varphi_2}^{\psi_1 \xi + \varphi_2} \left(C_3 A_i(t) + \left(C_4 + \frac{\Psi_3}{3} \right) B_i(t) \right) dt - \int_{\varphi_2}^{\psi_1 \eta + \varphi_2} \left(C_3 A_i(t) + \left(C_4 + \frac{\Psi_3}{3} \right) B_i(t) \right) dt \right), \text{ or } \int_\eta^\xi u_2(y) dy = \frac{1}{\psi_1} \left(\int_{\psi_1 \eta + \varphi_2}^{\psi_1 \xi + \varphi_2} \left(C_3 A_i(t) + \left(C_4 + \frac{\Psi_3}{3} \right) B_i(t) \right) dt \right), \tag{B.10}$$

where

$$\int_{\psi_1 \eta + \varphi_2}^{\psi_1 \xi + \varphi_2} A_i(t) dt = \int_{\psi_1 \eta + \varphi_2}^0 A_i(t) dt + \int_0^{\psi_1 \xi + \varphi_2} A_i(t) dt = - \int_0^{\psi_1 \eta + \varphi_2} A_i(t) dt + \int_0^{\psi_1 \xi + \varphi_2} A_i(t) dt. \tag{B.11}$$

Using asymptotic value of Airy's function from table-2 i.e. $\int_0^Z A_i(t) dt \approx \frac{1}{3}$ in Eq. (B.11), we get

$$\int_{\psi_1 \eta + \varphi_2}^{\psi_1 \xi + \varphi_2} A_i(t) dt = 0. \tag{B.12}$$

Similarly, we have

$$\int_{\psi_1 \eta + \varphi_2}^{\psi_1 \xi + \varphi_2} B_i(t) dt = \int_{\psi_1 \eta + \varphi_2}^0 B_i(t) dt + \int_0^{\psi_1 \xi + \varphi_2} B_i(t) dt = - \int_0^{\psi_1 \eta + \varphi_2} B_i(t) dt + \int_0^{\psi_1 \xi + \varphi_2} B_i(t) dt. \tag{B.13}$$

Using asymptotic value of Airy's function from table-2 i.e. $\int_0^Z B_i(t) dt \approx \frac{e^{2Z^{3/2}/3}}{\sqrt{\pi Z^{7/4}}}$ in Eq. (B.13), we get

$$\int_{\psi_1 \eta + \varphi_2}^{\psi_1 \xi + \varphi_2} B_i(t) dt = \frac{e^{\frac{2}{3}(\psi_1 \xi + \varphi_2)^{3/2}}}{\sqrt{\pi}(\psi_1 \xi + \varphi_2)^{7/4}} - \frac{e^{\frac{2}{3}(\psi_1 \eta + \varphi_2)^{3/2}}}{\sqrt{\pi}(\psi_1 \eta + \varphi_2)^{7/4}}. \tag{B.14}$$

Using Eq. (B.12) and Eq. (B.14) in Eq. (B.10), we get

$$\int_\eta^\xi u_2(y) dy = \frac{1}{\psi_1} \left(C_4 + \frac{\Psi_3}{3} \right) \left(\frac{e^{\frac{2}{3}(\psi_1 \xi + \varphi_2)^{3/2}}}{\sqrt{\pi}(\psi_1 \xi + \varphi_2)^{7/4}} - \frac{e^{\frac{2}{3}(\psi_1 \eta + \varphi_2)^{3/2}}}{\sqrt{\pi}(\psi_1 \eta + \varphi_2)^{7/4}} \right). \tag{B.15}$$

Now, $\int_\xi^1 u_3(y) dy$ can be written as below:

$$\int_{\xi}^1 u_3(y) dy = \int_0^1 u_3(y) dy - \int_0^{\xi} u_3(y) dy, \tag{B.16}$$

From Eq. (15), we have

$$\int_{\xi}^1 u_3(y) dy = \int_0^1 \left(C_5 A_i(\lambda_3 y + \varphi_3) + \left(C_6 + \frac{\Psi_4}{3} \right) B_i(\lambda_3 y + \varphi_3) \right) dy - \int_0^{\xi} \left(C_5 A_i(\lambda_3 y + \varphi_3) + \left(C_6 + \frac{\Psi_4}{3} \right) B_i(\lambda_3 y + \varphi_3) \right) dy. \tag{B.17}$$

Solving RHS of Eq. (B.17) by considering $t = \lambda_3 y + \varphi_3$, we have

$$\int_{\xi}^1 u_3(y) dy = \frac{1}{\lambda_3} \left(\int_{\varphi_3}^{\lambda_3 + \varphi_3} \left(C_5 A_i(t) + \left(C_6 + \frac{\Psi_4}{3} \right) B_i(t) \right) dt - \int_{\varphi_3}^{\lambda_3 \xi + \varphi_3} \left(C_5 A_i(t) + \left(C_6 + \frac{\Psi_4}{3} \right) B_i(t) \right) dt \right), \text{ or } \int_{\xi}^1 u_3(y) dy = \frac{1}{\lambda_3} \left(\int_{\lambda_3 \xi + \varphi_3}^{\lambda_3 + \varphi_3} \left(C_5 A_i(t) + \left(C_6 + \frac{\Psi_4}{3} \right) B_i(t) \right) dt \right), \tag{B.18}$$

where,

$$\int_{\lambda_3 \xi + \varphi_3}^{\lambda_3 + \varphi_3} A_i(t) dt = \int_{\lambda_3 \xi + \varphi_3}^0 A_i(t) dt + \int_0^{\lambda_3 + \varphi_3} A_i(t) dt = - \int_{\lambda_3 \xi + \varphi_3}^0 A_i(t) dt + \int_0^{\lambda_3 + \varphi_3} A_i(t) dt. \tag{B.19}$$

Using asymptotic value of Airy's function from table-2 i.e. $\int_0^Z A_i(t) dt \approx \frac{1}{3}$ in Eq. (B.19), we get

$$\int_{\lambda_3 \xi + \varphi_3}^{\lambda_3 + \varphi_3} A_i(t) dt = 0. \tag{B.20}$$

Similarly, we have

$$\int_{\lambda_3 \xi + \varphi_3}^{\lambda_3 + \varphi_3} B_i(t) dt = \int_{\lambda_3 \xi + \varphi_3}^0 B_i(t) dt + \int_0^{\lambda_3 + \varphi_3} B_i(t) dt = - \int_{\lambda_3 \xi + \varphi_3}^0 B_i(t) dt + \int_0^{\lambda_3 + \varphi_3} B_i(t) dt. \tag{B.21}$$

Using asymptotic value of Airy's function from table-2 i.e. $\int_0^Z B_i(t) dt \approx \frac{e^{2Z^{3/2}/3}}{\sqrt{\pi Z^{7/4}}}$ in Eq. (B.21), we get

$$\int_{\lambda_3 \xi + \varphi_3}^{\lambda_3 + \varphi_3} B_i(t) dt = \frac{e^{\frac{2}{3}(\lambda_3 + \varphi_3)^{3/2}}}{\sqrt{\pi}(\lambda_3 + \varphi_3)^{7/4}} - \frac{e^{\frac{2}{3}(\lambda_3 \xi + \varphi_3)^{3/2}}}{\sqrt{\pi}(\lambda_3 \xi + \varphi_3)^{7/4}}. \tag{B.22}$$

Using Eq. (B.20) and Eq. (B.22) in Eq. (B.18), we get

$$\int_{\xi}^1 u_3(y) dy = \frac{1}{\lambda_3} \left(C_6 + \frac{\Psi_4}{3} \right) \left(\frac{e^{\frac{2}{3}(\lambda_3 + \varphi_3)^{3/2}}}{\sqrt{\pi}(\lambda_3 + \varphi_3)^{7/4}} - \frac{e^{\frac{2}{3}(\lambda_3 \xi + \varphi_3)^{3/2}}}{\sqrt{\pi}(\lambda_3 \xi + \varphi_3)^{7/4}} \right). \tag{B.23}$$

Determination of arbitrary constants

On substituting all the values of velocities and stresses from the general solution of the problem into the boundary condition, we obtain a system of linear equations in arbitrary constants. This system is given by below matrix vector form:

$$AX = C, \tag{B.24}$$

where $X = \begin{bmatrix} C_1 \\ C_2 \\ C_3 \\ C_4 \\ C_5 \\ C_6 \end{bmatrix}$ is matrix of unknowns i.e. arbitrary constants to be evaluated for the particular solution of the present problem; $C =$

$$\begin{bmatrix} \frac{\pi P}{\lambda_1^2 M_{1\text{eff}}} N_i(\varphi_1) \\ \frac{\pi P}{\lambda_3^2 \alpha_2 M_{3\text{eff}}} N_i(\lambda_3 + \varphi_3) \\ \frac{\pi P}{\lambda_1^2 M_{1\text{eff}}} N_i(\eta\lambda_1 + \varphi_1) - \frac{\pi P}{\psi_1^2 \alpha_1 M_{2\text{eff}}} N_i(\eta\psi_1 + \varphi_2) \\ \frac{\pi P}{\psi_1^2 \alpha_1 M_{2\text{eff}}} N_i(\xi\psi_1 + \varphi_2) - \frac{\pi P}{\lambda_3^2 \alpha_2 M_{3\text{eff}}} N_i(\xi\lambda_3 + \varphi_3) \\ \frac{\pi P}{\lambda_1 M_{1\text{eff}}} N'_i(\eta\lambda_1 + \varphi_1) - \frac{\pi P}{\psi_1 M_{2\text{eff}}} N'_i(\eta\psi_1 + \varphi_2) \\ \frac{\pi P}{\psi_1 \alpha_1 M_{2\text{eff}}} N'_i(\xi\psi_1 + \varphi_2) - \frac{\pi P}{\lambda_3 \alpha_1 M_{3\text{eff}}} N'_i(\xi\lambda_3 + \varphi_3) \end{bmatrix}$$

is constant matrix vector and is coefficient matrix vector.

$$A = \begin{bmatrix} A_i(\varphi_1) & B_i(\varphi_1) & 0 & 0 & 0 & 0 \\ 0 & 0 & 0 & 0 & A_i(\lambda_3 + \varphi_3) & B_i(\lambda_3 + \varphi_3) \\ A_i(\eta\lambda_1 + \varphi_1) & B_i(\eta\lambda_1 + \varphi_1) - A_i(\eta\psi_1 + \varphi_2) - B_i(\eta\psi_1 + \varphi_2) & 0 & 0 & 0 & 0 \\ 0 & 0 & A_i(\xi\psi_1 + \varphi_2) & B_i(\xi\psi_1 + \varphi_2) - A_i(\xi\lambda_3 + \varphi_3) - A_i(\xi\lambda_3 + \varphi_3) & 0 & 0 \\ \lambda_1 A'_i(\eta\lambda_1 + \varphi_1) & \lambda_1 B'_i(\eta\lambda_1 + \varphi_1) - \alpha_1 \psi_1 A'_i(\eta\psi_1 + \varphi_2) - \alpha_1 \psi_1 B'_i(\eta\psi_1 + \varphi_2) & 0 & 0 & 0 & 0 \\ 0 & 0 & \psi_1 A'_i(\xi\psi_1 + \varphi_2) & \psi_1 B'_i(\xi\psi_1 + \varphi_2) - \frac{\alpha_2}{\alpha_1} \lambda_3 A'_i(\xi\lambda_3 + \varphi_3) - \frac{\alpha_2}{\alpha_1} \lambda_3 B'_i(\xi\lambda_3 + \varphi_3) & 0 & 0 \end{bmatrix}$$

Solving the above system of linear equations Eq. (B.24) in C_1, C_2, C_3, C_4, C_5 and C_6 with the help of MATHEMATICA 11.3, we get the values of arbitrary constants involved in the general solution of the present problem.

References

Abramowitz, M., Stegun, I., 1984. Handbook of Mathematical Functions. Dover, New York.

Allan, F.M., Hamdan, M.H., 2002. Fluid mechanics of the interface region between two porous layers. Appl. Math. Comput. 128 (1), 37–43.

Ansari, I.A., Deo, S., 2017. Effect of magnetic field on the two immiscible viscous fluids flow in a channel filled with porous medium. Natl. Acad. Sci. Lett. (India) 40 (3), 211–214.

Deo, S., Maurya, D.K., Filippov, A.N., 2020. Influence of magnetic field on micropolar fluid flow in a cylindrical tube enclosing an impermeable core coated with porous layer. Colloid J. 82 (6), 649–660.

Deo, S., Maurya, D.K., Filippov, A.N., 2021. Effect of magnetic field on hydrodynamic permeability of biporous membrane relative to micropolar liquid flow. Colloid J. 83 (6), 662–675.

Ford, R.A., Hamdan, M.H., 1998. Coupled parallel flow through composite porous layers. Appl. Math. Comput. 97 (2–3), 261–271.

Gulab, R., Mishra, R.S., 1977. Unsteady flow through magnetohydrodynamic porous media. Indian J. Pure Appl. Math. 8 (6), 637–647.

Hamdan, M.H., Kamel, M.T., 2011. Flow through variable permeability porous layers. Adv. Theor. Appl. Math. 4 (3), 135–145.

Hamdan, M.H., Kamel, M.T., Siyyam, H.I., 2009. A permeability function for Brinkman's equation. In WSEAS International Conference. Proceedings. Mathematics and Computers in Science and Engineering, 11 (198-205).

Happel, J., Brenner, H., 2012. Low Reynolds Number Hydrodynamics: with Special Applications to Particulate Media, vol. 1. Springer Science & Business Media.

Hill, A.A., Straughan, B., 2008. Poiseuille flow in a fluid overlying a porous medium. J. Fluid Mech. 603, 137–149.

Hou, J.S., Holmes, M.H., Lai, W.M., Mow, V., 1989. Boundary conditions at the cartilage-synovial fluid interface for joint lubrication and theoretical verifications. J. Biomech. Eng. 111, 78–87.

Jaiswal, S., Yadav, P.K., 2019. A micropolar-Newtonian blood flow model through a porous layered artery in the presence of a magnetic field. Phys. Fluids 31 (7), 071901.

Nield, Donald A., Adrian, Bejan, 2006. Convection in Porous Media, vol. 3. Springer, New York.

Nield, D.A., Kuznetsov, A.V., 2009. The effect of a transition layer between a fluid and a porous medium: shear flow in a channel. Transport Porous Media 78, 477–487.

Parvazinia, M., Nassehi, V., Wakeman, R.J., Ghoreishy, M.H.R., 2006. Finite element modeling of flow through a porous medium between two parallel plates using the brinkman equation. Transport Porous Media 63, 71–90.

Rudraiah, N., 1986. Flow past porous layers and their stability. In: Chermisinoff, N.P. (Ed.), Encyclopedia of Fluid Mechanics: Slurry Flow Technology. Gulf Publishing, Houston, pp. 567–647.

Srivastava, B.G., Deo, S., 2013. Effect of magnetic field on the viscous fluid flow in a channel filled with porous medium of variable permeability. Appl. Math. Comput. 219 (17), 8959–8964.

Vafai, K., Thiyagaraja, R., 1987. Analysis of flow and heat transfer at the interface region of a porous medium. Int. J. Heat Mass Tran. 30 (7), 1391–1405.

Wiegel, F.W., 1980. Fluid flow through porous macromolecular systems. In: Lecture Notes in Physics, No.121. Springer-Verlag, Berlin, Heidelberg, New York.

Yadav, P.K., 2013. Slow motion of a porous cylindrical shell in a concentric cylindrical cavity. Meccanica 48 (7), 1607–1622.

Yadav, P.K., 2018. Motion through a non-homogeneous porous medium: hydrodynamic permeability of a membrane composed of cylindrical particles. The European Physical Journal Plus 133 (1), 1.

Yadav, P.K., Jaiswal, S., 2018. Influence of an inclined magnetic field on the Poiseuille flow of immiscible micropolar-Newtonian fluids in a porous medium. Can. J. Phys. 96 (9), 1016–1028.

Yadav, P.K., Tiwari, A., Deo, S., Filippov, A., Vasin, S., 2010. Hydrodynamic permeability of membranes built up by spherical particles covered by porous shells: effect of stress jump condition. Acta Mech. 215 (1–4), 193–209.

Yadav, P.K., Deo, S., Yadav, M.K., Filippov, A., 2013. On hydrodynamic permeability of a membrane built up by porous deformed spheroidal particles. Colloid J. 75 (5), 611–622.

Yadav, P.K., Deo, S., Singh, S.P., Filippov, A., 2017. Effect of magnetic field on the hydrodynamic permeability of a membrane built up by porous spherical particles. Colloid J. 79 (1), 160–171.

Yadav, P.K., Jaiswal, S., Asim, T., Mishra, R., 2018a. Influence of a magnetic field on the flow of a micropolar fluid sandwiched between two Newtonian fluid layers through a porous medium. The European Physical Journal Plus 133 (7), 247.

Yadav, P.K., Jaiswal, S., Sharma, B.D., 2018b. Mathematical model of micropolar fluid in two-phase immiscible fluid flow through porous channel. Appl. Math. Mech. 39 (7), 993–1006.

Zaytoon, M.A., Alderson, T.L., Hamdan, M.H., 2016a. Flow over a Darcy porous layer of variable permeability. J. Appl. Math. Phys. 4 (1), 86.

Zaytoon, M.A., Alderson, T.L., Hamdan, M.H., 2016b. Flow through layered media with embedded transition porous layer. Int. J. of Enhanced Research in Science, Technology & Engineering 5 (4), 9–26.

Zaytoon, M.A., Alderson, T.L., Hamdan, M.H., 2016c. Flow through a layered porous configuration with generalized variable permeability. Int. J. of Enhanced Research in Science, Technology & Engineering 5 (6), 1–21.

Zaytoon, M.A., Alderson, T.L., Hamdan, M.H., 2016d. Flow through a variable permeability Brinkman porous core. J. Appl. Math. Phys. 4 (4), 766.

Zaytoon, M.A., Alderson, T.L., Hamdan, M.H., 2018. A study of flow through a channel bounded by a brinkman transition porous layer. J. Appl. Math. Phys. 6 (1), 264.